Research Article

Sinem Tunçer* and Rafig Gurbanov

A novel approach for the discrimination of culture medium from Vascular Endothelial Growth Factor (VEGF) overexpressing colorectal cancer cells

[Vasküler Endotelyal Büyüme Faktörünü (VEGF) aşırı ifade eden kolorektal kanser hücre kültür ortamının ayırt edilmesine yönelik yeni bir yaklaşım]

https://doi.org/10.1515/tjb-2020-0058
Received February 11, 2020; accepted March 26, 2020; published online June 29, 2020

Abstract

Objectives: The expression level of Vascular Endothelial Growth Factor (VEGF) is assumed as a prognostic marker for several tumor types, including colorectal cancer. Therefore, the determination of pre- and post-therapy levels of VEGF appears to have great value in the assessment of tumor prognosis. Enzyme-Linked Immunosorbent Assay (ELISA) is commonly used for the determination of serum or plasma VEGF levels, but the method is costly and time-consuming. In this study, we aimed to describe a rapid and cost-effective analysis method to discriminate VEGF overexpressing colorectal cancer-derived conditioned medium (CM).

Methods: Attenuated Total Reflection (ATR)-Fourier Transform Infrared (FTIR) spectroscopy, combined with Principal Component Analysis (PCA) and Linear Discriminant Analysis (LDA), was used to differentiate VEGF overexpressing colorectal cancer cell line CM from CM obtained from the corresponding control cells which express and secrete relatively lower amount of VEGF.

Results: Samples belong to VEGF overexpressing colorectal cancer cells were clearly distinguished from the control group with very high PC scores as PC1 + PC2 = 96%. Besides, a 100% accurate distinction between these two groups was achieved by the LDA analysis.

Conclusions: ATR-FTIR spectroscopy combined with pattern recognition techniques was able to discriminate CM of VEGF overexpressing colorectal cancer cells with high efficiency and accuracy.

Keywords: Attenuated Total Reflection (ATR)-Fourier Transform Infrared (FTIR) spectroscopy; Linear Discriminant Analysis (LDA); pattern recognition; Principal Component Analysis (PCA); Vascular Endothelial Growth Factor (VEGF); $VEGF_{165}$.

***Corresponding author: Sinem Tunçer**, Bilecik Seyh Edebali Universitesi, Vocational School of Health Services Department of Medical Laboratory Techniques, Pelitözü Mah. Fatih Sultan Mehmet Bulvarı No:27, Merkez, Bilecik, Turkey; and Bilecik Seyh Edebali Universitesi, Biotechnology Application and Research Center, Pelitözü Mah. Fatih Sultan Mehmet Bulvarı No:27, Merkez, Bilecik, Turkey, E-mail: sinem.tuncer@bilecik.edu.tr. https://orcid.org/0000-0002-8947-8646

Rafig Gurbanov: Bilecik Seyh Edebali Universitesi, Department of Molecular Biology and Genetics, Bilecik, Turkey; Bilecik Seyh Edebali Universitesi, Biotechnology Application and Research Center, Bilecik, Turkey. https://orcid.org/0000-0002-5293-6447

ÖZ

Amaç: Vasküler Endotelyal Büyüme Faktörünün (VEGF) ifade seviyesi, kolorektal kanser de dahil olmak üzere çeşitli tümör tipleri için prognostik bir belirteç olarak kabul

edilmektedir. Dolayısıyla, tümör prognozunun değerlendirilmesinde VEGF'nin tedavi öncesi ve sonrası düzeylerinin belirlenmesinin büyük bir değere sahip olduğu ortadadır. ELISA (Enzime Bağlı İmmünosorbent Deneyi) serum veya plazma VEGF düzeylerinin belirlenmesi için yaygın olarak kullanılır, ancak yöntem pahalı ve zaman alıcıdır. Bu çalışmada, aşırı VEGF ifade eden kolorektal kanser hücrelerinden elde edilen koşullu besiyerini (Conditioned medium-CM) ayırt edebilmek için hızlı ve uygun maliyetli bir analiz yönteminin tanımlanması amaçlanmıştır.

Yöntem: VEGF aşırı ifade eden kolorektal kanser hücrelerinden elde edilen CM'nin, görece daha az düzeyde VEGF ifade ve salınımı yapan kontrol hücrelerinden ayırt edilmesi amacı ile Temel Bileşen Analizi (PCA) ve Doğrusal Diskriminant Analizi (LDA), Attenuated Total Reflection (ATR)-Fourier Transform Infrared (FTIR) spektroskopisi ile birlikte kullanılmıştır.

Bulgular: Aşırı VEGF ifade eden kolorektal kanser hücrelerine ait örnekler, kontrol grubundan PC1 + PC2 = % 96 olmak üzere yüksek PC skorlarıyla ayırt edilebilmiştir. Ek olarak, LDA analizi ile bu iki grup arasında %100 doğrulukla ayrım sağlanmıştır.

Sonuç: Örüntü tanıma teknikleri ile analiz edilen ATR-FTIR spektroskopisi, VEGF'nin aşırı ifade edildiği kolorektal kanser hücrelerinden elde edilen CM'nin yüksek etkinlik ve doğrulukla ayırt edilebilmesini sağlamıştır.

Anahtar Kelimeler: Attenuated Total Reflection (ATR)-Fourier Transform Infrared (FTIR) spektroskopisi; Doğrusal Diskriminant Analizi (LDA); örüntü tanıma; Temel Bileşen Analizi (PCA); Vascular Endothelial Growth Factor (VEGF); $VEGF_{165}$.

Introduction

Blood vessels function in carrying nutrients to tissues and removing catabolic products. Therefore, the development of new blood and lymphatic vessels from the preexisting ones, called angiogenesis, serves vital homeostatic roles. On the other hand, uncontrolled growth of blood vessels can encourage or augment the severity of several diseases including cancer [1]. Vascular Endothelial Growth Factor (VEGF) plays a central role in the regulation of both vasculogenesis, the *de novo* formation of blood vessel networks through the differentiation of endothelial precursor cells, and angiogenesis [2].

The VEGF family comprises VEGF-A, VEGF-B, VEGF-C, VEGF-D, Placenta Growth Factor (PlGF), VEGF-E, and VEGF-F. VEGF-A is the most extensively studied member of this family [1]. VEGF proteins can interact with VEGF receptor (VEGFR)-1, VEGFR-2, VEGFR-3 and VEGF co-receptors Neuropilin (NP)-1 and NP-2 [3]. The triggered signaling pathways through these interactions can result in the proliferation, migration, and survival of the endothelial cells and new vessel formation involved in angiogenesis [4]. Although the VEGF research field is mainly occupied by the contributions of VEGF family members in angiogenesis and lymphangiogenesis, the roles of VEGF proteins are not confined to their abilities to promote or facilitate angiogenesis and vascular permeability [5]. For instance, these proteins can affect the immune response against tumor cells [6]. Besides, VEGF signaling can occur both in autocrine and paracrine manners in tumor cells and participate in key features of tumorigenesis apart from angiogenesis [5].

VEGF-A is the prototype member of the VEGF family of growth factors and referred to simply as VEGF [7, 8]. VEGF is expressed by various types of normal cells, but not surprisingly, its expression level has been shown to be elevated significantly in several malignant tumors, including colorectal cancer [5]. Dbouk et al. analyzed plasma VEGF levels 36 colorectal cancer patients by Enzyme-Linked Immunosorbent Assay (ELISA) and they found that the positive predictive value of VEGF was 89.5% [9]. Similarly, Akbulut et al. quantified serum VEGF levels of 52 colorectal cancer patients by ELISA and demonstrated that together with nitric oxide, the VEGF level was a prognostic factor of survival in patients with colorectal carcinoma. Furthermore, the authors investigated that an angiogenic index that relies on serum VEGF and nitrate concentrations can be considered a significant prognostic factor for disease-free survival (DFS) in patients with operable colorectal carcinoma [10]. Moreover, Tsai et al. examined VEGF expression in metastatic colorectal carcinoma patients before treatment and post-treatment with 5-fluorouracil and irinotecan combined with bevacizumab. The immunohistochemistry results showed that decreased peri-therapeutic VEGF expression can be used as a significant predictor of therapy response and can be used to predict six-month progression-free survival (PFS) [11]. Furthermore, De Vita et al. analyzed VEGF serum levels by ELISA in 81 patients with colon cancer in parallel with 50 healthy individuals and they found that higher preoperative serum VEGF concentrations were significantly correlated with shortened DSS and DFS. The authors suggested that serum VEGF levels

can be used to define patients who are suitable for curative surgery and enhanced VEGF levels after surgery can provide evidence for residual cancer, even though it was not macroscopically identified [12]. Besides being associated with poor prognosis, serum VEGF levels were also found to be significantly positively correlated with the size of the tumors in colorectal cancer patients [13]. Also, since VEGF expression has been demonstrated to be elevated in patients with metastatic tumors compared with non-metastatic tumors, VEGF expression level has been suggested to be used for the prediction of metastasis from colorectal carcinoma [14].

It is evident that the determination of pre- and post-operative or pre- and post-treatment VEGF levels seem to offer valuable prognostic information in colorectal carcinoma. ELISA is commonly used for the determination of VEGF serum or plasma levels, but performing ELISA assay for large numbers of patients is very expensive and time-consuming [15]. Herein, we aimed to describe a cost-effective and rapid analysis method using Attenuated Total Reflection (ATR)-Fourier Transform Infrared (FTIR) spectroscopy to differentiate the conditioned media (CM) obtained from VEGF overexpressing colorectal cancer cells without any requirement for extensive sample preparation steps. Today, utilization of spectroscopic techniques in biomedical research has significantly increased and more specifically, the use of spectroscopy in clinical studies has gained increasing attention from scientists. FTIR spectroscopy is a vibrational optical tool that can be applied for the detection of pathology-associated molecular alterations [16]. The obtained vibrational spectra produce the spectral fingerprint bands that are unique for the particular molecule and/or biological process [17]. It is a label-free, non-invasive, non-destructive, time-saving, simple and relatively inexpensive analytical technique based on the characterization of the biochemical profiles of samples without the need for extensive sample preparation steps [18, 19]. Principal Component Analysis (PCA) and Linear Discriminant Analysis (LDA) are pattern recognition techniques to reduce the complex FTIR spectral datasets of biological systems. Therefore, the combination of FTIR data with these pattern recognition techniques provides an excellent classification approach for the differentiation and classification of biological samples, including cancerous cells, with high accuracy [20–23]. In this study, FTIR spectroscopy coupled with PCA and LDA was used to discriminate VEGF overexpressing colorectal cancer cell line cell-free conditioned medium (CM) from the CM obtained from the control cells which express and secrete relatively lower amount of VEGF.

Materials and methods

Cell culture and treatments

HCT-116 cells, kindly provided by Dr. Sreeparna Banerjee from Middle East Technical University, were obtained from DSMZ-German Collection of Microorganisms and Cell Cultures (Germany) and cultured as described before [24]. Where indicated, HCT-116 cells were treated with tunicamycin (TM, Cell Signaling Technology, USA; 10 mg/mL stock in DMSO) or the corresponding amount of DMSO as vehicle control.

Cloning and transfections

The Human $VEGF_{165}$ coding sequence was cloned into pcDNA3.1(–) (Invitrogen, USA) through *XhoI* and *HindIII* by including Kozak sequence. Forward: 5′GGCCCTCGAGCCACCATGAACTTTCTGCTGTCTTGG3′ and Reverse: 5′ GGGAAGCTTTCACCGCCTCGGCTTGT3′ primers were used for $VEGF_{165}$ amplification from the template vector pcDNA-UTR-$VEGF_{165}$ which was provided by Dr. Ben Zion Levi from Israel Institute of Technology, Israel. The cloned vector was confirmed by sequencing.

To assess $VEGF_{165}$ overexpression, HCT-116 cells were plated as 5×10^5 cells/well on a 6-well plate. Day after, cells were transfected with empty pcDNA3.1(–) vector which is indicated as EV in the study, or with the $VEGF_{165}$ overexpression vector, called $VEGF_{165}$, by using X-tremeGENE HP (Roche, Mannheim, Germany) transfection agent.

Immunocytochemistry

The day before the transfection, cells were plated on 12-well plate containing pre-sterilized coverslips. Transfections were done as mentioned above. Twenty-four hours after transfection, cells were fixed at room temperature (RT) for 15 min with 3.7% formaldehyde. Followed by washing steps, cells were incubated for 10 min with methanol at −20 °C for permeabilization. After washing, blocking was done by incubating the coverslips with 3% (g/mL) Bovine Serum Albumin at RT for 30 min. After the blocking step, cells were incubated for 45 min in the VEGF-A antibody (Cat no: ab46154; Abcam, UK). At the end of incubation, the antibody was removed and cells were washed. As a fluorescently labeled secondary antibody, anti-rabbit secondary antibody (Cat no: A-11008; Thermo Fisher Scientific, USA), conjugated with Alexa Fluor 488 was used. Cells were incubated at RT for 30 min with the secondary antibody. After removal of the secondary antibody, coverslips were incubated for 30 min at RT with 1 µg/mL Propidium iodide (PI) and 1 µg/mL RNaseA for nuclear staining. The samples were examined under Leica DMI4000 with Andor DSD2 Spinning Disc Confocal Microscope (Leica Microsystems, Germany).

Western blotting

Western blot experiments were carried out as described previously [24]. Membranes were incubated with VEGF-A antibody (Cat no: ab46154; Abcam, UK). Anti-rabbit IgG-HRP secondary antibody (Cat no: R-05072-500A; Advansta, USA) was used against the VEGF-A antibody. β-actin (Cat no: sc-47778; Santa Cruz Biotechnology, USA) was chosen as a loading control. HRP-conjugated Anti-mouse secondary antibody (Cat no: R-

05071-500; Advansta) was used against β-actin antibody. Clarity Western ECL Substrate (Bio-Rad, USA) was applied to detect protein bands.

Determination of VEGF secretion

Quantikine Human VEGF Immunoassay (R&D Systems, USA) Enzyme-linked Immunosorbent Assay (ELISA) kit was used according to the manufacturer's instructions.

ATR-FTIR spectroscopic data acquisition and processing

HCT-116 cells were transfected for 24 h with $VEGF_{165}$ overexpression vector or EV as described above. After 24 h, the transfection medium was discarded and the cells were further incubated for 24 h in complete growth medium (RMPI-1640 medium containing 1% penicillin/streptomycin, 2 mM L-glutamine, and 10% FBS) with or without TM. DMSO was used as vehicle control. To obtain CM, followed by incubation with TM or vehicle, the medium was collected and centrifuged at 4 °C, 125 × g for 10 min. After centrifugation, CM were transferred to new eppendorf tubes for spectroscopic analyses. The spectra of CM were obtained using Frontier FTIR Spectrometer (PerkinElmer, US) equipped with a universal ATR Miracle accessory. The spectrum of air was used as a reference. 10 µL of CM was placed on a ZnSe crystal plate (PerkinElmer, US). Complete RPMI-1640 medium was scanned under identical scanning conditions as the samples and the spectrum of the medium were subtracted manually from the spectra of the samples using the Spectrum 100 software (PerkinElmer, US). To eliminate the effect of the medium, the free water band located around 2,125 cm^{-1} was flattened using the same software. The obtained difference spectra were used for all further analyses. Two biological replicates of each CM group with two technical replicates were analyzed. The samples were scanned in the spectral range between 4,000 and 650 cm^{-1} at RT with a resolution of 4 cm^{-1} and the spectra were collected as an average of 32 scans.

Discrimination of dataset using unsupervised PCA

PCA was applied to the mean-centered difference spectra in the whole (4,000–650 cm^{-1}) infrared region via The Unscrambler X 10.4 (Camo, NO) software [25]. Full Cross Validation method, Singular Value Decomposition algorithm, and Hotelling's T2 statistics were used in the model.

Classification of the dataset using supervised LDA

By using The Unscrambler X 10.4 software [25], LDA was applied to spectral data (4,000–650 cm^{-1}) as described previously [24]. Assuming equal prior probabilities, the Quadratic classifiers method was used following defining the data for modeling.

Statistical data analysis

The results are represented as mean ± standard error of the mean (SEM). Statistical analyses were carried out in Prism 6.01 (GraphPad, USA). *t*-test was applied to compare two groups (*$p \le 0.05$, **$p \le 0.01$, ***$p \le 0.001$, ****$p \le 0.0001$).

Results

Overexpression of $VEGF_{165}$ in colorectal cancer cells enhanced intracellular and secreted VEGF

The human *VEGF* gene has four main splice isoforms. Among them, the 165 amino acid long isoform, namely $VEGF_{165}$, has been shown to display the strongest mitogenic response [26]. HCT-116 colorectal cancer cells were transfected with either EV or $VEGF_{165}$ vector to assess $VEGF_{165}$ overexpression. 24 h post-transfection, cells were stained with VEGF antibody to detect intracellular VEGF. As can be seen in Figure 1A, VEGF can be detected in EV transfected cells and overexpression was successful since HCT-116 cells expressing a higher amount of $VEGF_{165}$ were distinguished by immunocytochemistry. Analysis of secreted VEGF amount by ELISA in both EV and $VEGF_{165}$ transfected HCT-116 cells showed that overexpression not only increased intracellular VEGF accumulation but also enhanced the secreted VEGF amount (Figure 1B). Intracellular VEGF was also analyzed by western blot at 24 and 48 h post-transfection. As it is shown in Figure 1C, under denaturing conditions, two bands were detected in the $VEGF_{165}$ overexpressing HCT-116 cells. Since VEGF is known as a heavily glycosylated dimeric protein with a molecular weight of 36–46 kDa [27], the higher molecular weight band, shown by an asterisk, was likely to be the glycosylated form of the $VEGF_{165}$ monomer. To understand whether the band was representing the glycosylated form of the protein, followed by 24 h transfection with $VEGF_{165}$ overexpression vector, the cells were treated with an N-glycosylation inhibitor TM for 24 h. TM treatment eliminated the upper band, indicating that the slower-migrating protein correlates with the glycosylated form of $VEGF_{165}$ monomer (Figure 2).

FTIR spectroscopy, coupled with PCA and LDA, displays clear discrimination of CM obtained from VEGF overexpressing colorectal cancer cells

PCA aids to transform a group of equivalent variables into a smaller set of distinct variables called principal components (PCs). Therefore, a reduced size PC model can be employed to identify and distinguish abnormalities/deviations rapidly in the original system [20, 28]. In this study, we applied this model to FTIR spectral data to achieve a straightforward differentiation of the CM collected

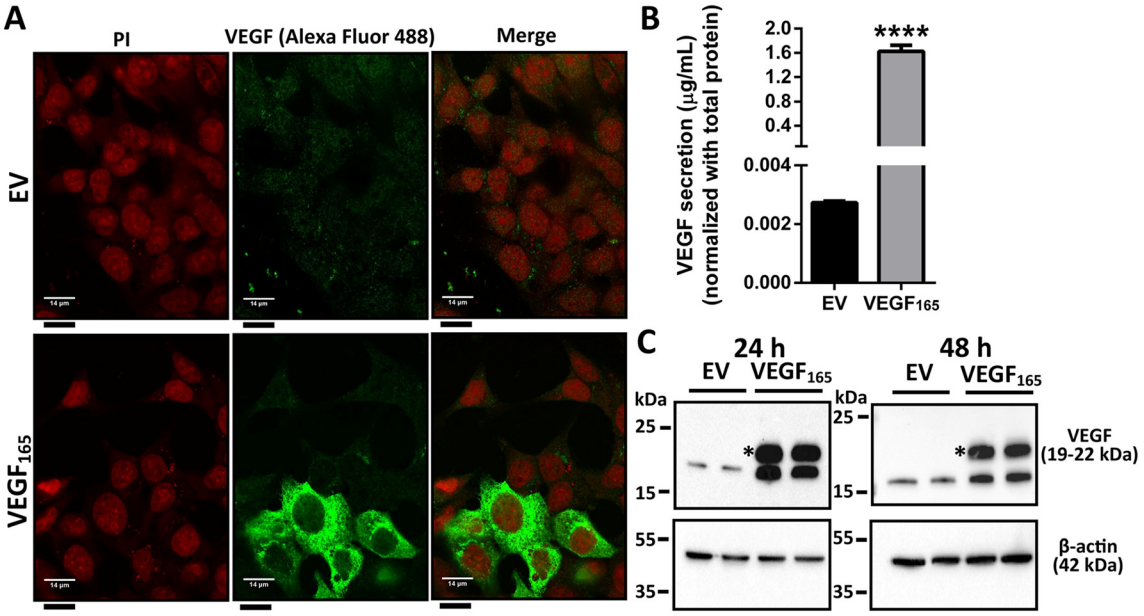

Figure 1: $VEGF_{165}$ overexpression in colorectal cancer cells. HCT-116 cells were transiently transfected with EV or $VEGF_{165}$ overexpression vector and (A) The intracellular level and distribution of VEGF were observed by immunofluorescence staining after transient transfection for 24 h. Alexa Fluor 488 labeled (green) secondary antibody was used to detect VEGF and PI staining was used to detect the nucleus. Each scale bar represents 14 µm. (B) Secreted VEGF amounts in the CM collected from EV or $VEGF_{165}$ transfected cells were determined by ELISA after 24 h transfection. The results belong to two independent biological replicates each with two technical replicates. (C) VEGF expression was determined by western blot following 24 and 48 h transfection. *: higher molecular weight $VEGF_{165}$ monomer.

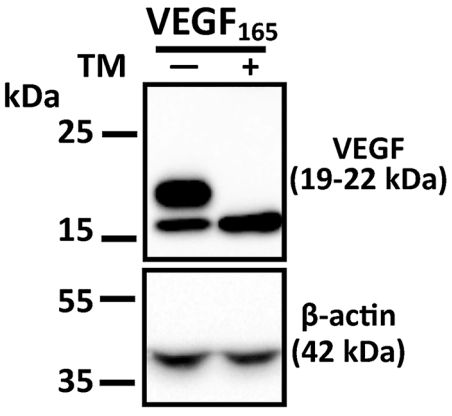

Figure 2: $VEGF_{165}$ is glycosylated in colorectal cancer cells. Following 24 h transfection, $VEGF_{165}$ transfected HCT-116 cells were treated with TM or with DMSO (vehicle) for 24 h. A higher molecular weight band disappeared with TM treatment.

from VEGF overexpressing cells (VEGF group) from the CM of EV transfected cells (EV group). As can be seen from the scores plot (Figure 3A), the VEGF group was clearly distinguished from the EV group with very high PC scores (PC1 + PC2 = 96%). Of note, the VEGF group located at the left (negative) side of the plot whereas the EV group resided at the right (positive) side of the plot.

The explained variance plot measures how much information is taken into account by each PC and it is expressed as a percentage of the global variance in the data. Accordingly, the explained variance of a variable is the fraction of the global variance of the variable taken into account by the model. The calibration variance relies on fitting the calibration data to the model. The validation variance is computed by testing the model on data that was not used in model building. When the difference between these variances is large, it should be questioned whether the calibration data or the test data is representative [25]. Calibration and validation curves of variables, i. e., PCs, were presented in explained variance plot (Figure 3B) to demonstrate the most influential variables (PC1/81% and PC2/15%) and the equivalent patterns of calibrated and validated variances.

LDA provides a linear transformation of n-dimensional feature samples into an m-dimensional space ($m < n$) and by maximizing the differences between the predefined classes concerning the new variable, the same class members cluster together while members of different classes cluster separately [24, 29]. A 100% accurate distinction between VEGF and EV groups was achieved by the LDA analysis (Figure 4A). The numerical data for this classification was provided as confusion, prediction, and classification matrices. Without any

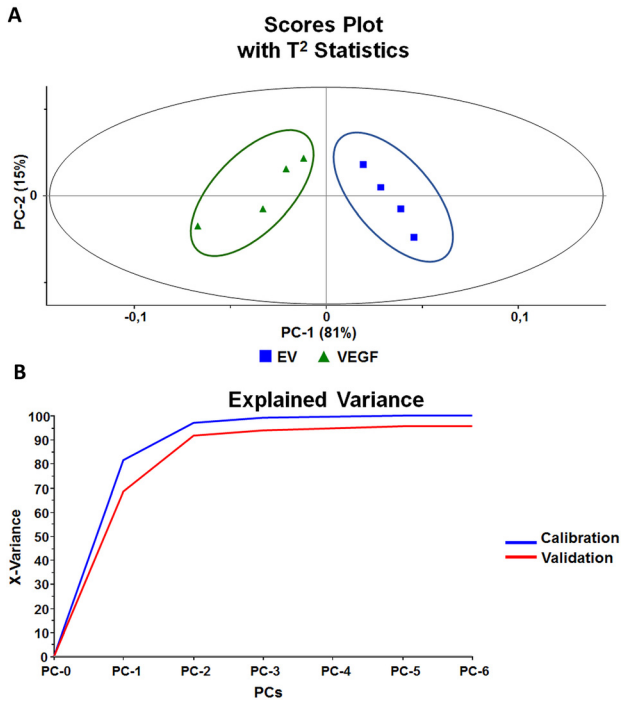

Figure 3: The differentiation of CM obtained from VEGF overexpressing colorectal cancer cells by unsupervised PCA. (A) Scores plot with Hotelling's T^2 limit obtained at 4,000–650 cm^{-1} spectral region for EV and VEGF groups. (B) Explained variance plot, obtained for the error, measures how much information is considered by each PCs by means of calibration (blue-colored) and validation (red-colored) curves.

confusion (Figure 4B), the model perfectly predicted each sample in its corresponding group (Figure 4C). The classification matrix of the dataset also confirmed the model (Figure 4D).

We then tested if this methodology can also be used for the discrimination of TM treated cells. We analyzed FTIR spectra from the CM samples obtained from (i) EV transfected cells treated with vehicle (EV group), (ii) EV transfected cells treated with TM (EV-TM group), (iii) $VEGF_{165}$ transfected cells treated with vehicle (VEGF group), and (iv) $VEGF_{165}$ transfected cells treated with TM (VEGF-TM group). A sharply defined differentiation of all the above-mentioned groups was achieved with high PC scores (PC1 + PC2 = 99%) (Figure 5A). It was seen that the EV group placed at the lower-right side of the scores plot while an intense accumulation towards the upper-right side of the plot observed for EV-TM group. VEGF group was found to be positioned at the mid-central region of the plot although the VEGF-TM group was situated at the left (negative) side of the plot. Showing the most effective variables (PC1/95% and PC2/4%), identical calibration and validation curves of PCs were presented in Figure 5B.

Finally, LDA was performed to ATR-FTIR spectra of EV, EV-TM, VEGF, and VEGF-TM groups (Figure 6). The discrimination plot of the analysis revealed that the groups flatly classified with 100% accuracy (Figure 6A). Confusion (Figure 6B), prediction (Figure 6C), and classification matrices (Figure 6D) of the obtained numerical data signify the exact prediction and classification of the samples in their corresponding groups without any confusion.

Discussion

Overexpression of VEGF has been shown in several tumors and it appears to be an independent prognostic marker for several tumor types including colorectal cancer [30, 31]. Ishigami et al. showed that in colorectal cancer patients, VEGF expression level is correlated with the progression, invasion, and metastasis of colorectal cancer, and its overexpression is closely associated with poor prognosis [31]. Although ELISA is a commonly used method to detect serum/plasma VEGF levels, it is a tedious/laborious, expensive, and time-consuming method. Besides, the detection is based on the enzyme/substrate reaction so the readout must be obtained in a short time [32]. In the manuscript, we aimed to investigate if pattern recognition/modeling algorithms applied to FTIR spectra can be used to distinguish samples obtained from VEGF overexpressing colorectal cancer cells. For this purpose, we overexpressed $VEGF_{165}$ isoform in human colorectal cancer cell line HCT-116, since it is the predominant isoform of VEGF and commonly found to be elevated in a variety of solid human tumors [33]. PCA and LDA analyses were applied to the FTIR spectra of the cell-free CM obtained from $VEGF_{165}$ overexpressing or EV transfected control cells. Both analyses revealed a clear distinction and classification between these two groups. Presumably, this distinction and classification caused not only by the secreted VEGF but also by the changes in the secretome, a collection of proteins secreted into the extracellular space, due to enhanced intracellular VEGF expression [34]. In breast cancer cell line derived xenograft models, Dore-Savard et al. were identified clear differences between the tumor microenvironments (TME) of xenografts with or without VEGF overexpression and showed the role of VEGF in modifying the angiogenic secretome [34]. Since TME plays roles in tumor growth, angiogenesis and metastasis, there has recently been an increased interest in this subfield of tumor biology [35]. Tumor secretome contains critically important factors of the TME which shape the outcome of tumor initiation,

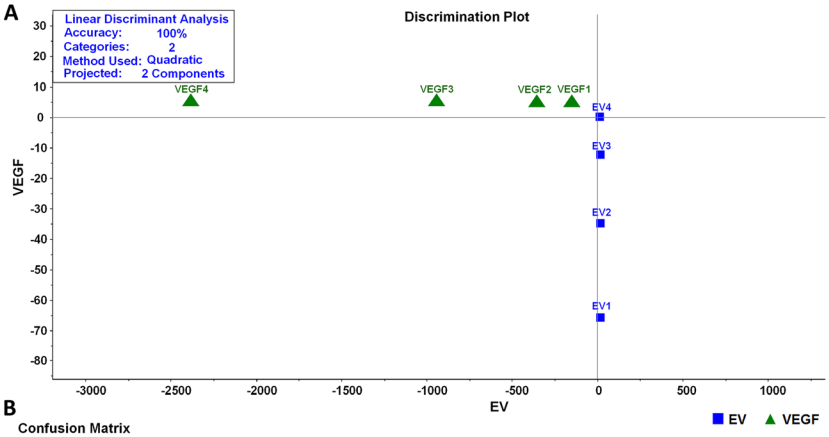

B Confusion Matrix

Confusion	Actual	EV	VEGF
Predicted		1	2
EV	1	4	0
VEGF	2	0	4

C Prediction Matrix

Prediction		EV	VEGF	Predicted
		1	2	3
EV1	1	8,6657	-64,2958	EV
EV2	2	8,7583	-33,6005	EV
EV3	3	9,6939	-11,7724	EV
EV4	4	8,9954	0,9799	EV
VEGF1	5	-173,9255	7,4831	VEGF
VEGF2	6	-360,7251	7,7086	VEGF
VEGF3	7	-954,7304	6,8607	VEGF
VEGF4	8	-2405,8640	6,8863	VEGF

D Classification Matrix

Classified		EV	VEGF	Class
		1	2	3
EV1	1	8,6657	-64,2958	EV
EV2	2	8,7583	-33,6005	EV
EV3	3	9,6939	-11,7723	EV
EV4	4	8,9954	0,9799	EV
VEGF1	5	-173,9255	7,4831	VEGF
VEGF2	6	-360,7245	7,7086	VEGF
VEGF3	7	-954,7307	6,8607	VEGF
VEGF4	8	-2405,8600	6,8863	VEGF

Figure 4: The classification of CM obtained from VEGF overexpressing colorectal cancer cells by supervised LDA. (A) The discrimination plot obtained at 4,000–650 cm^{-1} spectral region for EV and VEGF groups. (B) Confusion, (C) prediction, and (D) classification matrices for EV and VEGF groups.

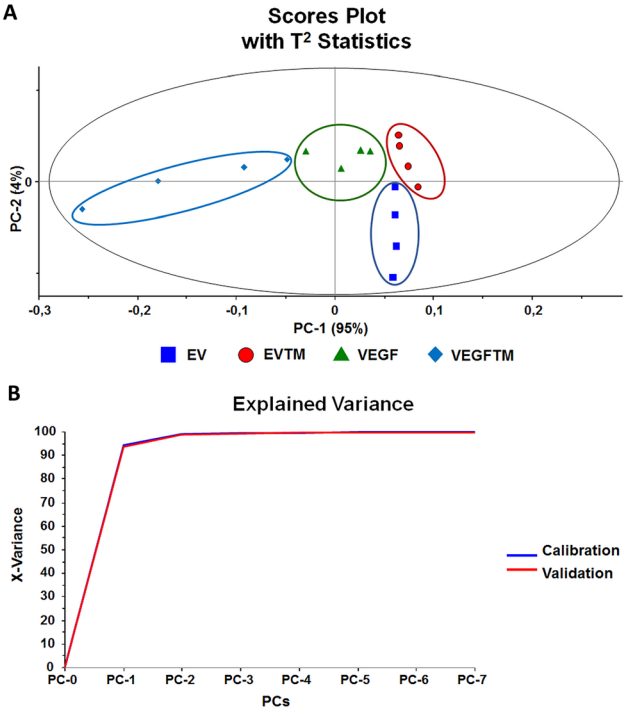

Figure 5: The differentiation of CM obtained from TM treated HCT-116 cells by PCA. (A) Scores plot with Hotelling's T2 limit obtained at 4,000–650 cm^{-1} spectral region for for the experimental groups. (B) Calibration (blue-colored) and validation (red-colored) curves for explained variance.

progression and contain a collection of regulatory molecules identifying the biochemical and physical microenvironment of cancer cells and therefore determine the response to tumor treatment [34,35]. Our results revealed that FTIR spectroscopy can be used as a powerful tool to distinguish TME with different characteristics and therefore can be evaluated as a new analysis method for the identification of tumor interstitial fluid samples based on tumor VEGF expression levels.

In this manuscript, we also showed that FTIR spectroscopy coupled with PCA and LDA approaches was also able to discriminate TM treated samples from untreated counterparts. Although a distinct borderline between VEGF and EV-TM groups was obvious, these two groups were located within relative proximity to one another. As an N-glycosylation inhibitor, TM causes endoplasmic reticulum stress resulted from protein misfolding [36]. Very recently, we have shown that TM treatment enhances VEGF expression and secretion in different types of cancer cells, including colorectal cancer cells [37]. Therefore, closer proximity of the VEGF group to EV-TM group, in terms of the distance between these groups, may indicate an elevated VEGF expression and secretion level in EV transfected cells caused by TM treatment.

In sum, FTIR spectroscopy coupled with PCA and LDA can be used to identify VEGF overexpressing

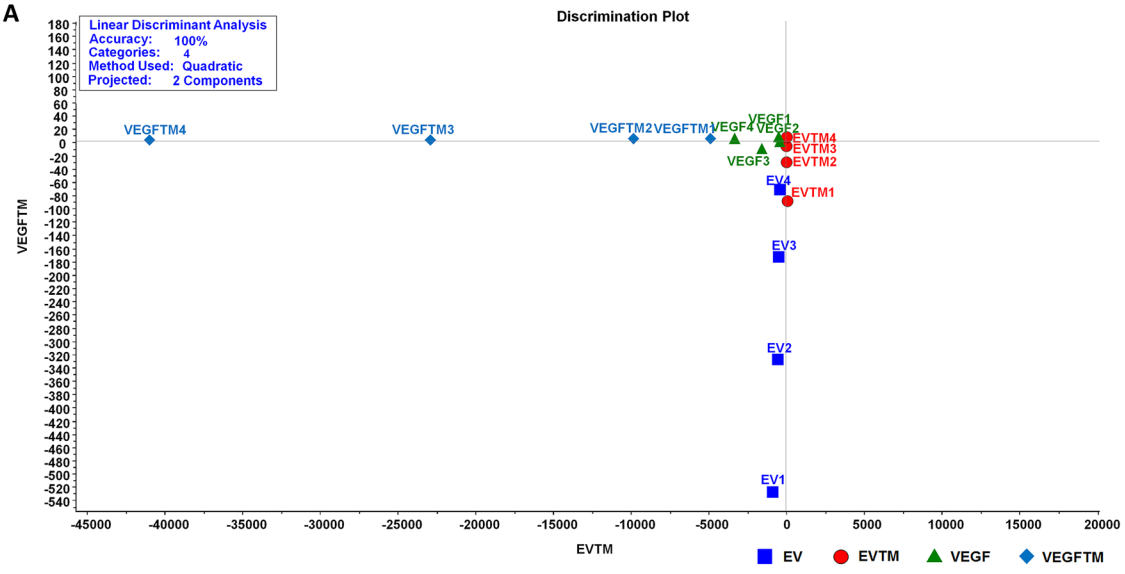

B

Confusion Matrix

Confusion matrix	Actual	EV	EVTM	VEGF	VEGFTM
Predicted		1	2	3	4
EV	1	4	0	0	0
EVTM	2	0	4	0	0
VEGF	3	0	0	4	0
VEGFTM	4	0	0	0	4

C

Prediction Matrix

Prediction		EV	EVTM	VEGF	VEGFTM	Predicted
		1	2	3	4	5
EV1	1	7,9889	-1197,7670	-89,0182	-520,7127	EV
EV2	2	8,1091	-640,9993	-47,1204	-323,1312	EV
EV3	3	9,0165	-354,6477	-17,5142	-169,8220	EV
EV4	4	8,3119	-153,4730	-0,8163	-71,4440	EV
EVTM1	5	-129,8013	8,7941	-2,5593	-85,5144	EVTM
EVTM2	6	-36,0703	9,4889	3,9562	-31,6779	EVTM
EVTM3	7	4,2111	8,9478	5,1401	-0,9790	EVTM
EVTM4	8	5,6546	8,5943	3,3248	4,1444	EVTM
VEGF1	9	-201,9743	-370,8953	6,9894	0,0357	VEGF
VEGF2	10	-396,2166	-626,9329	7,1677	2,5438	VEGF
VEGF3	11	-933,3500	-1677,4800	6,3503	-9,5184	VEGF
VEGF4	12	-2538,9860	-3370,8110	6,3753	6,2140	VEGF
VEGFTM	13	-3653,5000	-5005,3620	5,4579	6,3319	VEGFTM
VEGFTM	14	-7044,0690	-9553,6070	1,0066	6,8531	VEGFTM
VEGFTM	15	-17170,6800	-23005,8400	-15,7607	5,9749	VEGFTM
VEGFTM	16	-29717,2000	-41096,9000	-46,5061	5,8871	VEGFTM

D

Classification Matrix

Classified_		EV	EVTM	VEGF	VEGFTM	Class
		1	2	3	4	5
EV1	1	7,9888	-1197,7760	-89,0183	-520,7132	EV
EV2	2	8,1091	-640,9979	-47,1204	-323,1313	EV
EV3	3	9,0165	-354,6467	-17,5142	-169,8219	EV
EV4	4	8,3119	-153,4725	-0,8163	-71,4440	EV
EVTM1	5	-129,8019	8,7941	-2,5593	-85,5144	EVTM
EVTM2	6	-36,0701	9,4889	3,9562	-31,6778	EVTM
EVTM3	7	4,2113	8,9477	5,1401	-0,9790	EVTM
EVTM4	8	5,6546	8,5942	3,3247	4,1444	EVTM
VEGF1	9	-201,9752	-370,8972	6,9894	0,0357	VEGF
VEGF2	10	-396,2169	-626,9332	7,1677	2,5438	VEGF
VEGF3	11	-933,3502	-1677,4810	6,3503	-9,5184	VEGF
VEGF4	12	-2538,9890	-3370,8140	6,3753	6,2140	VEGF
VEGFTM1	13	-3653,4980	-5005,3590	5,4579	6,3319	VEGFTM
VEGFTM2	14	-7044,0560	-9553,5890	1,0066	6,8531	VEGFTM
VEGFTM3	15	-17170,700	-23005,870	-15,7607	5,9748	VEGFTM
VEGFTM4	16	-29717,210	-41096,930	-46,5062	5,8871	VEGFTM

Figure 6: The classification of CM obtained from TM treated cells by LDA. (A) The discrimination plot obtained at 4,000–650 cm^{-1} spectral region for EV, EV-TM, VEGF, and VEGF-TM groups. (B) Confusion, (C) prediction, and (D) classification matrices for the experimental groups.

epithelial cells through analyzing growth medium instead of using conventional methods aiming to analyze intracellular VEGF expression (i. e., western blotting, qRT-PCR, immunocytochemistry) and/or VEGF secretion (i. e., ELISA). Besides, this method has the potential to be used as a new approach to discriminate the characteristics of serum/plasma samples either from colon cancer patients or patients with other types of tumors depending on VEGF expression levels. Although further studies comprising the sufficient number of patient samples with known VEGF expression levels and clinicopathological factors are needed, our results suggest that FTIR spectra can be applied to triage or stratify the patients with tumors. As preprocessing steps in machine learning, PCA and LDA methods applied to FTIR spectra would ideally fit the needs of clinics being cost-saving and rapid approaches.

Acknowledgments: The authors thank Bilecik Seyh Edebali University, Biotechnology Application and Research Center for providing laboratory facilities. The authors would like gratefully to thank Dr. Sreeparna Banerjee

(Department of Biological Sciences, Middle East Technical University) for sharing resources.

Research funding: This research did not receive any specific grant.

Author contributions: All authors have accepted responsibility for the entire content of this manuscript and approved its submission.

Competing interests: The authors declare that there is no conflict of interest regarding the publication of this article.

References

1. Apte RS, Chen DS, Ferrara N. VEGF in signaling and disease: beyond discovery and development. Cell 2019;176:1248–64.
2. Kolte D, McClung JA, Aronow WS. Vasculogenesis and angiogenesis. Transl Res Coronary Artery Dis Pathophysiol Treatment 2016;117:3–32.
3. Koch S, Claesson-Welsh L. Signal transduction by vascular endothelial growth factor receptors. Cold Spring Harb Perspect Med 2012;437:169–83.
4. Abhinand CS, Raju R, Soumya SJ, Arya PS, Sudhakaran PR. VEGF-A/VEGFR2 signaling network in endothelial cells relevant to angiogenesis. J Cell Commun Signal 2016;10:347–54.
5. Goel HL, Mercurio AM. VEGF targets the tumour cell. Nat Rev Cancer 2013;13:871–82.
6. Hansen W, Hutzler M, Abel S, Alter C, Stockmann C, Kliche S, et al. Neuropilin 1 deficiency on CD4+Foxp3+ regulatory T cells impairs mouse melanoma growth. J Exp Med 2012;209:2001–16.
7. Patel-Hett S , D'Amore PA. Signal transduction in vasculogenesis and developmental angiogenesis. Int J Dev Biol 2011;55:353–63.
8. Yang J, Yan J, Liu B. Targeting VEGF/VEGFR to modulate antitumor immunity. Front Immunol 2018;9:1–9.
9. Dbouk H, Tawil A, Nasr F, Kandakarjian L, Abou-Merhi R. Significance of CEA and VEGF as diagnostic markers of colorectal cancer in lebanese patients. Open Clin Cancer J 2007; 1:1–5.
10. Akbulut H, Altuntas F, Akbulut KG, Ozturk G, Cindoruk M, Unal E, et al. Prognostic role of serum vascular endothelial growth factor, basic fibroblast growth factor and nitric oxide in patients with colorectal carcinoma. Cytokine 2002;20:184–90.
11. Tsai HL, Lin CH, Huang CW, Yang IP, Yeh YS, Hsu W-H, et al. Decreased peritherapeutic VEGF expression could be a predictor of responsiveness to first-line FOLFIRI plus bevacizumab in mCRC patients. Int J Clin Exp Pathol 2005;8:1900–10. 25973082.
12. De Vita F, Orditura M, Lieto E, Infusino S, Morgillo F, Martinelli E, et al. Elevated perioperative serum vascular endothelial growth factor levels in patients with colon carcinoma. Cancer 2004;100:270–8.
13. Pangarsa EA, Suharti C, Santosa D, Setiawan B, Ulthofiah A. The correlation between serum vascular endothelial growth factor (VEGF) levels and size of colorectal cancer tumors. Hiroshima J Med Sci 2018;67:97–100.
14. Martins SF, Garcia EA, Luz MAM, Pardal F, Rodrigues M, Filho AL. Clinicopathological correlation and prognostic significance of VEGF-A, VEGF-C, VEGFR-2 and VEGFR-3 expression in Colorectal cancer. Cancer Genom Proteom 2013;10:55–67. 23603341.
15. Wang X, Dong L, Liang Y, Ni H, Tang J, Xu C, et al. Performance evaluation of FlowCytomix assays to quantify cytokines in patients with rheumatoid arthritis. Int J Clin Exp Med 2015;9:16158–66. 26629129.
16. Ellis DI, Goodacre R. Metabolic fingerprinting in disease diagnosis: Biomedical applications of infrared and Raman spectroscopy. Analyst 2006;131:875–85.
17. Talari ACS, Martinez MAG, Movasaghi Z, Rehman S, Rehman IU. Advances in Fourier transform infrared (FTIR) spectroscopy of biological tissues. Appl Spectrosc Rev 2017;52:456–506.
18. Butler HJ, Brennan PM, Cameron JM, Finlayson D, Hegarty MG, Jenkinson MD, et al. Development of high-throughput ATR-FTIR technology for rapid triage of brain cancer. Nat Commun 2019;10: 4501.
19. Gurbanov R, Yıldız F. Molecular profile of oral probiotic bacteria to be used with functional foods. J Food Heal Sci 2017;3:117–31.
20. Gurbanov R, Gozen AG, Severcan F. Rapid classification of heavy metal-exposed freshwater bacteria by infrared spectroscopy coupled with chemometrics using supervised method. Spectrochim. Acta Part A Mol Biomol Spectrosc 2018;189: 282–90.
21. Khanmohammadi M, Bagheri Garmarudi A, Samani S, Ghasemi K, Ashuri A. Application of linear discriminant analysis and attenuated total reflectance fourier transform infrared microspectroscopy for diagnosis of colon cancer. Pathol Oncol Res 2011;17:435–41.
22. Theophilou G, Lima KMG, Martin-Hirsch PL, Stringfellow HF, Martin FL. ATR-FTIR spectroscopy coupled with chemometric analysis discriminates normal, borderline and malignant ovarian tissue: classifying subtypes of human cancer. Analyst 2016;141:585–94.
23. Zlotogorski-Hurvitz A, Dekel BZ, Malonek D, Yahalom R, Vered M. FTIR-based spectrum of salivary exosomes coupled with computational-aided discriminating analysis in the diagnosis of oral cancer. J Cancer Res Clin Oncol 2019;145:685–94.
24. Tunçer S, Gurbanov R, Sheraj I, Solel E, Esenturk O, Banerjee S. Low dose dimethyl sulfoxide driven gross molecular changes have the potential to interfere with various cellular processes. Sci Rep 2018;8:14828.
25. Multiple Linear Regression. In: The Unscrambler X User Manual, Camo software Inc, Woodbridge, NJ, USA, 2014, pp. 583–616.
26. Keyt BA, Berleau LT, Nguyen H V., Chen H, Heinsohn H, Vandlen R, et al. The carboxyl-terminal domain (111-165) of vascular endothelial growth factor is critical for its mitogenic potency. J Biol Chem 1996;271:7788–95.
27. de Oliveira Dias JR, de Andrade GC, Novais EA, Farah ME, Rodrigues EB. Fusion proteins for treatment of retinal diseases: Aflibercept, ziv-aflibercept, and conbercept. Int J Retin Vitr 2016;2:3.
28. Gurbanov R, Simsek Ozek N, Gozen AG, Severcan F. Quick discrimination of heavy metal resistant bacterial populations using infrared spectroscopy coupled with chemometrics. Anal Chem 2015;87:9653–61.
29. Gurbanov R, Tunçer S, Mingu S, Severcan F, Gozen AG. Methylation, sugar puckering and Z-form status of DNA from a heavy metal-acclimated freshwater Gordonia sp. J Photochem Photobiol B Biol 2019;198:111580.
30. De Fraipont F, El Atifi M, Gicquel C, Bertagna X, Chambaz EM, Feige JJ. Expression of the angiogenesis markers vascular endothelial growth factor-A, thrombospondin-1, and platelet-derived endothelial cell growth factor in human sporadic

adrenocortical tumors: Correlation with genotypic alterations. J Clin Endocrinol Metab 2000;85:4734–41.
31. Ishigami SI, Arii S, Furutani M, Niwano M, Harada T, Mizomoto M, et al. Predictive value of vascular endothelial growth factor (VEGF) in metastasis and prognosis of human colorectal cancer. Br J Cancer 1998;78:1379–84.
32. Hosseini S, Vázquez-Villegas P, Rito-Palomares M, Martinez-Chapa SO. Advantages, disadvantages and modifications of conventional ELISA, Enzyme-Linked Immunosorbent Assay (ELISA), SpringerBriefs in Applied Sciences and Technology. Singapore: Springer; 2018; pp. 68–9.
33. Alvarez RH, Guarneri V, Icli F, Johnston S, Khayat D, Loibl S, et al. Bevacizumab treatment for advanced breast cancer. Oncologist 2011;16:1684–97.
34. Dore-Savard L, Lee E, Kakkad S, Popel AS, Bhujwalla ZM. The angiogenic secretome in VEGF overexpressing breast cancer xenografts. Sci Rep 2016;6:39460.
35. Wiig H, Tenstad O, Iversen PO, Kalluri R, Bjerkvig R. Interstitial fluid: the overlooked component of the tumor microenvironment? Fibrogenesis Tissue Repair 2010;3:1–11.
36. Guha P, Kaptan E, Gade P, Kalvakolanu D V, Ahmed H. Tunicamycin induced endoplasmic reticulum stress promotes apoptosis of prostate cancer cells by activating mTORC1. Oncotarget 2017;8:68191–207.
37. Tunçer S, Solel E, Banerjee S. Extensive unfolded protein response stimulation in colon cancer cells enhances VEGF expression and secretion. BSEU J Sci 2020;7: 329–43.